

基于时空最优低维动力系统的多尺度 可压缩湍流数值模拟方法*

齐 进¹, 吴锤结²

(1. 北京应用物理与计算数学研究所, 北京 100088;
2. 大连理工大学 力学与航空航天学院, 辽宁 大连 116024)

(我刊编委吴锤结来稿)

摘要: 按照周培源教授关于研究湍流数值模拟建模时必须分析和求解脉动速度场的思想, 该研究基于第一性原理, 系统地建立了基于时空低维最优动力系统的多尺度可压缩湍流数值模拟方法 (LMS 方法), 并将其应用于多次冲击 Richtmyer-Meshkov 问题的数值模拟中, 首次得到了可压缩湍流的中尺度流场和不同于 DNS 近似解的湍流近似解. 数值结果表明, LMS 方法可以用较少的网格获得更精确的湍流近似解. 首先解决了研究中遇到的几个问题, 为 LMS 方法的构建铺平了道路. 这些问题是: 基于湍流的物理特性, 提出了湍流大、中、小尺度分解的新概念; 找到了 box 滤波空间相关性的计算方法; 指出了湍流建模理论中长期存在的逻辑错误, 提出了多尺度湍流模型的概念; 讨论了湍流封闭问题的本质和关键, 给出了克服湍流封闭问题的数值方法. 采用 box 滤波方法/空间网格平均方法且在大尺度网格的意义下, LMS 方法的本质是一种将 RANS、LES、DES 和 DNS 等湍流数值模拟方法统一的全新湍流数值模拟方法. 需要指出的是, LMS 方法也可以作为湍流模型研究的辅助工具, 以检验 SGS 尺度方程/脉动方程中各项所对应的湍流模型是否正确.

关键词: 周培源对湍流研究的开拓性贡献; 时空最优低维动力系统; LMS 方法; 多尺度湍流模型; 可压缩湍流

中图分类号: O35 文献标志码: A DOI: 10.21656/1000-0887.440294

LMS Method: a Spatiotemporal Optimal Low-Dimensional Dynamical Systems of Multi-Scale Numerical Simulation Method for Compressible Turbulence

QI Jin¹, WU Chuijie²

(1. Institute of Applied Physics and Computational Mathematics, Beijing 100088, P.R.China;
2. School of Mechanics and Aerospace Engineering, Dalian University of Technology,
Dalian, Liaoning 116024, P.R.China)

(Contributed by WU Chuijie, M. AMM Editorial Board)

Abstract: Following Professor P-Y CHOU's idea, i.e., to study numerical simulation of turbulence, it is necessary to analyse and solve the fluctuating velocity field, based on the first principles, the spatiotemporal low-dimensional optimal

* 收稿日期: 2023-09-28; 修订日期: 2023-11-03

作者简介: 齐进 (1977—), 女, 副研究员 (E-mail: qi_jin@iapcm.ac.cn);

吴锤结 (1955—), 男, 教授 (通讯作者. E-mail: cjwudut@dlut.edu.cn).

引用格式: 齐进, 吴锤结. 基于时空最优低维动力系统的多尺度可压缩湍流数值模拟方法[J]. 应用数学和力学, 2024, 45(3): 318-336.

dynamical systems of multi-scale simulation method (LMS method) is established systematically in this work, and in its application to the numerical simulation of re-shock Richtmyer-Meshkov problem, the turbulent middle-scale flow field and an approximate solution of turbulence which is different from the DNS approximate solution of turbulence, are obtained for the first time; the numerical results show that LMS method can be used with fewer grids to obtain more accurate approximate solutions of turbulence. Several problems encountered in the research are solved first, which paved the road to construct LMS method. These problems are: based on the physical characteristics of turbulence, a new concept of large, middle and small scale decomposition of turbulence is proposed; calculation method of spatial correlation of box filtering is found; a long-standing logical error in the theory of turbulence modelling is pointed out and the concept of multi-scale turbulence models is suggested; essence and key of closure problem of turbulence are discussed and numerical method for overcoming the closure problem of turbulence is given. With the box filtering/the space grid average and in the sense of a large-scale grid, the essence of the LMS method is a new turbulence numerical simulation method that integrates the RANS, LES, DES and DNS. It is necessary to indicate that the LMS method can also serve as an auxiliary tool for turbulence model research to examine whether the turbulence model corresponding to each term in the SGS-scale/fluctuations equation is correct or not.

Key words: P-Y CHOU's pioneering contribution to turbulence research; spatiotemporal optimal low-dimensional dynamical systems; LMS method; multiscale turbulence models; compressible turbulence

1 Professor P-Y CHOU's Pioneering Contribution to Turbulence Research and the Basic Idea of the LMS Method

1.1 P-Y CHOU's Pioneering Contribution to Turbulence Research

Professor P-Y CHOU, the father of computational modeling^[1], published a groundbreaking paper^[2] on turbulence modeling in *Chinese Journal of Physics* in 1940, in which he proposed that to study the numerical simulation of turbulence, it is necessary to analyze and solve the fluctuating velocity field. He first presented the second- and third-order velocity correlation equations. Then, he transformed the fourth-order correlation function into a closure equation by summing the product of two second-order correlation functions. This process is the foundation of turbulence modeling theory. However, it is not the best method for computationally modeling turbulence (see section 4).

1.2 Basic Ideas of the LMS Method

In this report, for clarity, we present the term “small-scale” as “SGS-scale” in the LES method, and in the LMS method (see section 2), the SGS-scale includes middle-scale and small-scale.

Following Chou's idea, based on first principles, with the box filtering and without the Favre filter and any artificial assumption, coupled with the LES equation, a set of spatiotemporal multiscale optimal low-dimensional dynamical systems equations is solved with a small-scale turbulent model to obtain the middle-scale flow field, together with the LES large-scale averaged flow field to obtain a new kind of approximate solution of turbulence.

In this report, several problems encountered in the research and their solutions are studied first, as shown in section 2 to section 5. Then, the LMS method is established systematically in section 6, and its application on the re-shock Richtmyer-Meshkov problem is discussed in section 6.3. Finally, concluding remarks are given in section 7.

2 Classification of the Numerical Simulation Methods of Turbulence and Basic Features of the LMS Method

2.1 Classification of Numerical Simulation Methods of Turbulence From the Point View of Scale Decomposition

Traditional numerical simulation methods of turbulence include RANS^[3], LES^[4], DES^[5] and DNS^[6]. We used

the following categories to classify the numerical simulation methods of turbulence from the point view of scale decomposition.

1) Class L(Large): All scales of turbulence are solved by CFD methods to obtain a unified solution of turbulence f , such as DNS.

2) Class LS(Large-Small): The turbulence flow field is decomposed into large-scale and SGS-scale fields. The large-scale equation is solved by the CFD method, and the SGS-scale equation can be solved by:

- ① Coupling the solution of the CFD method with the large-scale equation;
- ② Coupling the dynamic system or optimal low-dimensional dynamic system method with the large-scale equation;
- ③ Using the SGS model in the LES equation.

Class LS includes the RANS, LES and DES methods, and the numerical results are large-scale averaged solutions of turbulence \bar{f} .

$$f = \bar{f} + f'. \quad (1)$$

Since the SGS-scale in class LS includes a wavenumber range with completely different turbulence characteristics, it is not easy to find accurate turbulence models in RANS, LES and DES.

3) Class LMS(Large-Middle-Small)

It can be seen from [fig. 1](#) that for high Reynolds number turbulence, the Kolmogorov spectra can be divided into the energy-containing range and the universal equilibrium range, in which the inertial sub-range is dominated by convection and dissipation is very small. Moreover, the dissipation range in which most turbulent energy is dissipated. Therefore, according to the basic characteristics of turbulence, the whole range of the turbulence spectrum wavenumbers can be divided into three parts with completely different characteristics, i.e., the energy-containing range, the inertial subrange and the dissipation range.

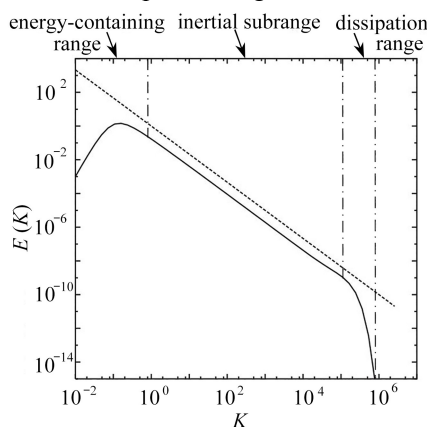


Fig. 1 Basic characteristics of turbulence

According to the basic characteristics of turbulence, the approximate solution of the turbulence f is divided into three parts as in equation (2): large-scale averaged quantities \bar{f} , middle-scale quantities f' and small-scale quantities f'' .

$$f = \bar{f} + f' + f''. \quad (2)$$

Class LMS includes the LMS(Low-dimensional dynamical systems Multiscale Simulation) method (see section 6).

2.2 Basic Features of the LMS Method

Large-scale quantities \bar{f} reflect the characteristics of the energy-containing range, which are related to specific

turbulence problems and must be obtained by solving a large-scale equation using the CFD method. The SGS term in the large-scale equation includes the middle-scale SGS correlation term and the role of the small-scale SGS turbulence model. \bar{f} reflects the characteristics of the energy-containing range, which are related to specific turbulence problems.

The middle-scale quantities f' reflect the convection characteristics of the anisotropic inertial subrange, which is obtained with the spatiotemporal optimal low-dimensional dynamical system equation. This equation includes large- and middle-scale quantities, with the large-scale equation in the middle-scale grid $\Delta x/2^p, p \geq 1$.

Since the dissipation range contains most of the dissipation effects of turbulence, the small-scale quantities are very small and isotropic, and the grid sizes in the dissipation range are very small, it is not suitable for direct solving. The effects of small-scale quantities f'' are found by a small-scale SGS turbulence model expressed by the middle-scale quantities together with the middle-scale deformation tensor and the large-scale stress tensor, which provides an appropriate dissipation effect.

3 Average and Filtering Operations and Calculation of Spatial Correlation of Box Filtering

In this section, we clarify the concepts of average and filtering operations and the correlation operation related to the box filter used in the LMS method.

3.1 Average and Filtering Operation

The following are the definitions of RANS and LES, in which the key concepts are the averaging operations (RANS) and filtering operations (LES).

RANS: by using turbulence averaging operations (including the time average, spatial average, ensemble average, etc.), the flow variables are decomposed into mean and fluctuating quantities.

LES: by using turbulence filtering operations (including the box filter, Fourier filter, Gaussian filter, etc.), the flow variables are decomposed into large-scale quantities and SGS-scale quantities.

3.1.1 Filtering Method

The given filtering function $G(|\mathbf{x} - \mathbf{y}|)$ is used to decompose the flow variables into large-scale $\overline{f(\mathbf{x}, t)}$ and SGS-scale quantities $f'(\mathbf{x}, t)$ as follows:

$$\begin{cases} f(\mathbf{x}, t) = \overline{f(\mathbf{x}, t)} + f'(\mathbf{x}, t), \\ \overline{f(\mathbf{x}, t)} = \int_{\Omega} G(|\mathbf{x} - \mathbf{y}|) f(\mathbf{y}, t) d\Omega, \\ f' = f - \overline{f}. \end{cases} \quad (3)$$

3.1.2 Box Filter

The filtering function of the box filter for the grid scale Δx_i is

$$G(|\mathbf{x} - \boldsymbol{\xi}|) = \begin{cases} \frac{1}{\Delta x_1 \Delta x_2 \Delta x_3}, & \text{if } |x_i - \xi_i| \leq \frac{\Delta x_i}{2}, i = 1, 2, 3. \\ 0, & \text{others,} \end{cases} \quad (4)$$

As shown in [fig. 2](#), the box filter is the volume average on the grid centered around \mathbf{x} . In RANS, the grid space averaging is equivalent to the box filtering. Therefore, only the RANS and LES in DES use grid space averaging, then, the DES is determined to be conceptually correct. Since generally, the averaging (RANS) and the filter (LES) used in the DES method are not compatible with each other, therefore the DES method is conceptually wrong, even though sometimes good results of turbulence numerical simulation can be obtained.

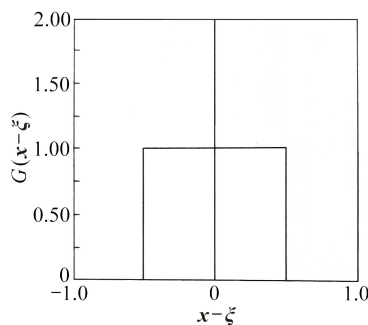


Fig. 2 Box filter: flat top hat filter

3.2 Variable Correlation and Spatiotemporal Correlation, Calculation of Spatial Correlation of Box Filtering

3.2.1 Variable Correlation

Correlation function: the average or filter of the self-multiplication of the same or different fluctuating or SGS-scale quantities are generally not equal to zero, and their values are related to the degree of correlation between these two fluctuating or SGS-scale quantities.

$$\begin{cases} \overline{a'b'} > 0, & \text{positive correlation,} \\ \overline{a'b'} < 0, & \text{negative correlation,} \\ \overline{a'b'} = 0, & \text{non correlation.} \end{cases} \quad (5)$$

Correlation coefficient: using the correlation coefficient R to measure the degree of correlation between a', b' yields

$$R = \frac{\overline{a'b'}}{\sqrt{\overline{a'^2} \overline{b'^2}}}. \quad (6)$$

If $R = \pm 1$, then they are completely correlated. It can be seen that each fluctuating or SGS-scale quantity is completely related to itself.

3.2.2 Spatiotemporal Correlation and the Calculation of the Spatial Correlation of the Box Filtering

Since we do not use time-averaged functions in this study, only spatial correlations are studied.

In spatial correlations, for a grid, when the distance is equal to 0, its spatial correlation coefficient is equal to 1; for an infinite distance, its spatial correlation coefficient is equal to 0.

Therefore, the spatial correlation coefficient of the box filtering is equal to 1 for this grid and is equal to 0 for other grids. Thus, the spatial correlation of the box filtering in the LMS method can be clearly calculated.

3.3 Correlation Functions With RANS and SGS Models

The above discussion shows that it is important to calculate the spatial correlations in coupling to solve LES+SGS equations; therefore, two questions arise:

- 1) How can we represent the effects of the correlation functions in the RANS and SGS models?
- 2) Furthermore, are the RANS/SGS models independent of the averaging (RANS) or filtering (LES) operations used in turbulence numerical simulations?

4 Errors in the Theoretical Basis of Turbulence Modeling and Multiscale Turbulence Models

4.1 Basic Consensus and Abbreviation Conventions

To establish the bases for the following discussion, we first provide two basic statements:

Consensus 1 Under a coarse grid, it is impossible to obtain turbulence with a numerical simulation of the Navier-Stokes equation.

Consensus 2 Only with the DNS grid can complete turbulence be obtained with the numerical simulation of the Navier-Stokes equation.

Second, the following abbreviation conventions are used in the discussion.

We let the arbitrary mathematical equation be $A = 0, B = 0$, and apply a function $(\bar{\quad})$ to A to obtain $\bar{A} = 0$ and $A - \bar{A} = B = 0$.

For the turbulence study, we let the Navier-Stokes equation be $A = 0$.

For RANS: the Reynolds average operation is defined as $(\bar{\quad})$, the Reynolds average equation is $\bar{A} = \text{RANS} = 0$, and the fluctuation equation is $A - \bar{A} = \text{FLUC} = 0$.

For LES: the filtering operation is defined as $(\bar{\quad})$, the large-eddy equation is $\bar{A} = \text{LES} = 0$, and the SGS-scale equation is $A - \bar{A} = \text{SGS} = 0$.

4.2 Theoretical Basis of the Classical Turbulence Modeling and the Logic Problem

We take the LES as an example in the discussion. The results are the same as those of the RANS.

If the LES and SGS equations are coupled solving in the LES grid, i.e.

$$\text{Coupled solution of LES and SGS: } \begin{cases} \text{LES} = 0, & \text{with LES grid,} \\ + \quad \rightarrow \text{NS} = 0, & \text{with LES grid,} \\ \text{SGS} = \text{NS} - \text{LES} = 0, & \text{with LES grid.} \end{cases} \quad (7)$$

Then, since from Consensus 1, we know that turbulence cannot be calculated by the Navier-Stokes equation in the LES grid; therefore, the coupled solution of the LES+SGS equations in the LES grid or the single-scale SGS model that approximates the SGS equation has a logic problem.

That is, in the coupled solution of LES+SGS equations, the closer the result is to $\text{SGS} = 0$, the less turbulent the solution is, i.e., there is a contradiction between the purpose and result, which means there is a logical error; or in the modeling, we cannot make $\text{SGS} = 0$, then, the so-called turbulent results come from unphysical errors of modeling and/or numerical algorithms, which is absurd.

4.3 Correct Theoretical Basis of Turbulence Modeling and Multiscale Turbulence Models

The basis of correct turbulence modeling theory is equation+grids.

To obtain complete turbulence, the DNS grid must be used with the Navier-Stokes equation.

$$\text{Coupled solution of LES+SGS: } \begin{cases} \text{LES} = 0, & \text{with LES grid,} \\ + \quad \rightarrow \text{similar to NS} = 0, & \text{with DNS grid,} \\ \text{SGS} = \text{NS} - \text{LES} = 0, & \text{with small-scale grid,} \end{cases} \quad (8)$$

i.e., a multiscale turbulence model must be used in LES to obtain correct turbulent results.

Notably, since the SGS equation is different from the Navier-Stokes equation used in DNS, the solution of the SGS equation, i.e., the so-called SGS-scale flow field, is conceptually different from the small-scale flow structures obtained by DNS.

However, the amount of computation required to solve the SGS equation on the SGS-scale grid is enormous, even exceeding that of DNS. Therefore, we must develop a new method (see section 6).

Finally, we noticed that this type of “modeling” method also appears in other disciplines, so such logic errors widely exist.

5 Essence and Key of the Closure Problem of Turbulence and Numerical Method for Overcoming the Closure Problem of Turbulence

5.1 Essence and Key of the Closure Problem of Turbulence

The closure problem of turbulence is a long-standing unsolved problem in the theoretical bases of turbulence modeling. It is very important to understand the essence and key of the closure problem of turbulence. The closure problem of turbulence can be stated as follows: when constructing the equation of the SGS-scale correlation terms,

there will be more higher-order SGS-scale correlation terms produced in each order of the equation of SGS-scale correlation terms.

First, the closure problem of turbulence is produced in the study of numerical simulation and modeling of turbulence; therefore, the essence of it is not a theoretical problem but a numerical problem.

Second, the key to the closure problem of turbulence is the requirement of the simultaneity of the SGS-scale and the SGS-scale correlation terms, which is similar to the following basic philosophy problem: did the chicken or the egg come at the same time?

Since the Reynolds stress equation of the RANS or LES comes from the fluctuation equation or SGS equation, it is not necessary to study the Reynolds stress equation but only to use a numerical method to couple the RANS+fluctuation equations or LES+SGS equations to overcome the closure problem of turbulence numerically.

5.2 Numerical Method for Overcoming the Closure Problem of Turbulence

The method of alternating coupling solutions of the LES and SGS equations is adopted, and the SGS-scale terms obtained at the last moment are used to calculate the SGS-scale correlation terms so that the SGS-scale and SGS-scale correlation terms are not simultaneous. Therefore, the closure problem of turbulence can be overcome with a numerical method.

In fact, in 2000 and 2009, we successfully applied the alternating coupling solution method of the LES equation and POD low-dimensional dynamical system equation in the numerical simulation of incompressible turbulence^[7-8].

6 LMS Method for Numerical Simulation of Compressible Turbulence

After overcoming the problems in section 2, section 3, section 4 and section 5, we can now develop the LMS method for the numerical simulation of compressible turbulence.

In the LMS method, the most important innovation is the application of a spatiotemporal multiscale optimal low-dimensional dynamical system of the middle-scale equation to ensure the accuracy of middle-scale turbulence modeling.

6.1 Predictability of Low-Dimensional Dynamical Systems and Spatiotemporal Intrinsic Bases

In a previous paper^[9] on the spatiotemporal optimal low-dimensional dynamical system, there are important findings, such as those shown in fig. 3. In general, low-dimensional dynamical systems with a spatial bases, such as cases of the first eight legends in fig. 3 are not predictive, i.e., the solution errors increase with time, and the spatiotemporal optimal low-dimensional dynamical system with a spatiotemporal intrinsic bases, such as the case of last legend in fig. 3 is predictable, i.e., the solution errors can be neglected.

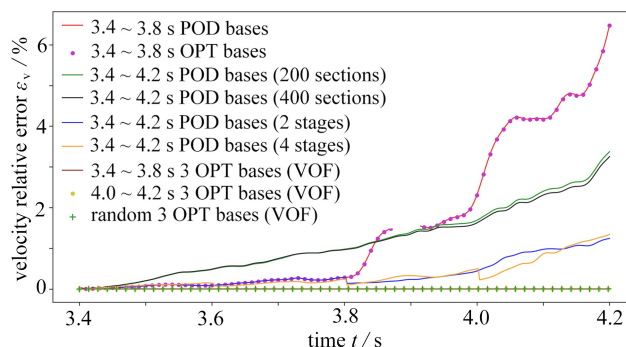


Fig. 3 Predictability of low-dimensional dynamical systems ($N=30$, $Re=2000$)

Note To get the meanings of different colors in the figure, the readers could refer to the electronic webpage of this article.

The key point is the spatiotemporal intrinsic bases $\xi_k(\mathbf{x}, t)$, which characterizes the spatiotemporal characteristics of the system. The approximated optimal solution space can be spanned with the spatiotemporal intrinsic bases that advances with time and forms the spatiotemporal optimal low-dimensional dynamical system

with the lowest N , which will be used as the spatiotemporal optimal low-dimensional dynamical system of the middle-scale equation.

$$\mathbf{u}(\mathbf{x}, t) = \mathbf{u}_N + \mathbf{u}_R \approx \sum_{k=1}^N a_k(t) \boldsymbol{\xi}_k(\mathbf{x}, t). \quad (9)$$

6.2 LMS Method for the Numerical Simulation of Compressible Turbulence

6.2.1 Dimensional Compressible Turbulence Large-Scale Equation

The state equation is

$$p = \rho R_g T, \quad (10)$$

where R_g is the universal gas constant ($R_g = 287.0$). The dimensional compressible Navier-Stokes equation is

$$\begin{cases} \rho_{,t} + (\rho u_j)_{,j} = 0, \\ (\rho u_i)_{,t} + (\rho u_i u_j + p \delta_{ij})_{,j} - \sigma_{ij,j} = 0, \\ E_{,t} + [(E + p)u_j]_{,j} - \kappa T_{,jj} - (\sigma_{ij} u_i)_{,j} = 0, \end{cases} \quad (11)$$

where E is total energy,

$$E \equiv \frac{p}{(\gamma - 1)\gamma Ma^2} + \frac{1}{2} \rho (u_h u_h), \quad (12)$$

where the specific heat ratio is $\gamma = 1.4$ and Ma is the Mach number.

Since there are drawbacks with the Favre filter, we do not use the Favre filter in the LMS method. We applied the box filter to the dimensional compressible Navier-Stokes equation (11), to obtain the dimensional compressible turbulence large-scale equation.

$$\begin{cases} \bar{\rho}_{,t} + (\bar{\rho} \bar{u}_j)_{,j} + r_{j,j} + \mathcal{R}_{j,j} = 0, \\ (\bar{\rho} \bar{u}_i + r_i)_{,t} + (\bar{\rho} \bar{u}_i \bar{u}_j)_{,j} + \bar{p}_{,i} - \bar{\sigma}_{ij,j} + \tau_{ij,j} + \mathcal{T}_{ij,j} = 0, \\ \bar{E}_{,t} + (\bar{E} \bar{u}_j)_{,j} + (\bar{p} \bar{u}_j)_{,j} - (\bar{u}_i \bar{\sigma}_{ij})_{,j} - \kappa \bar{T}_{,jj} + q_{j,j} + C_v \mathcal{Q}_{j,j} = 0. \end{cases} \quad (13)$$

r_j , τ_{ij} and q_j are middle-scale correlation terms of the LMS method,

$$\begin{cases} r_j = \overline{\rho u_j} - \bar{\rho} \bar{u}_j = \overline{\rho' u'_j}, \\ \tau_{ij} = \overline{\rho u_i u_j} - \bar{\rho} \bar{u}_i \bar{u}_j = \overline{\rho' u'_i u'_j} + \overline{u_i \rho' u'_j} + \overline{u_j \rho' u'_i} + \overline{\rho' u'_i u'_j}, \\ q_j = \overline{(E + p)u_j} - (\bar{E} + \bar{p}) \bar{u}_j - \overline{\sigma_{ij} u_i} + \overline{\sigma_{ij} \bar{u}_i} = \overline{(E' + p')u'_j} - \overline{\sigma'_{ij} u'_i}. \end{cases} \quad (14)$$

\mathcal{T}_{ij} is the small-scale SGS Reynolds stress tensor, $\mathcal{T}_{ij} = \overline{\rho''(u'_i u'_j - \bar{u}''_i \bar{u}''_j)}$, and the small-scale Smagorinsky SGS model based on middle-scale quantities is

$$\mathcal{T}_{ij} - \frac{\delta_{ij}}{3} \mathcal{T}_{kk} = -2\nu_t \bar{S}_{ij} = -2C_s^2 \Delta^2 |\bar{S}'| \bar{S}_{ij}, \quad (15)$$

where $|\bar{S}'| = \sqrt{2\bar{S}'_{ij}\bar{S}'_{ij}}$ is the modulus of middle-scale strain rate tensor, $\nu_t = C_s^2 \Delta^2 |\bar{S}'|$ is the eddy viscosity, and \bar{S}_{ij} is the large-scale strain rate tensor.

\mathcal{R}_j is the small-scale SGS turbulence mass flux, $\mathcal{R}_j = \overline{\rho'' u''_j}$. Its small-scale SGS turbulence mass flux model is

$$\mathcal{R}_j = \overline{\rho'' u''_j} = -C_s^2 \Delta^2 |\bar{S}'| \frac{\partial \bar{\rho}}{\partial x_j}. \quad (16)$$

\mathcal{Q}_j is the small-scale SGS heat flux term:

$$\mathcal{Q}_j = \nu_t C_p Pr T. \quad (17)$$

6.2.2 Equations of the Middle-Scale Dynamical System of Compressible Turbulence

Navier-Stokes equation – large-scale equation = middle-scale equation:

$$\left\{ \begin{aligned} & \rho'_{,t} = (\overline{\rho' u'_j} - \overline{\rho} u'_j - \rho' u'_j - \rho' \overline{u_j})_{,j}, \\ & (\overline{\rho u'_i} + \rho' \overline{u_i} + \rho' u'_i - \overline{\rho' u'_i})_{,t} = \left[-\overline{\rho u'_i u'_j} - \overline{\rho} u'_i u'_j - \overline{\rho' u'_i u'_j} - \rho' \overline{u_i u_j} - \rho' \overline{u_i} u'_j - \rho' u'_i \overline{u_j} - \rho' u'_i u'_j + \right. \\ & \quad \left. \overline{\rho u'_i u'_j} + \overline{u_i} \overline{\rho' u'_j} + \overline{u_j} \overline{\rho' u'_i} + \overline{\rho' u'_i u'_j} - R_g \delta_{ij} (\overline{\rho} T' + \rho' \overline{T} + \rho' T' - \overline{\rho' T'}) + \mu \left(u'_{i,j} + u'_{j,i} - \frac{2}{3} \delta_{ij} u'_{h,h} \right) \right]_{,j}, \\ & \left[\frac{R_g}{\gamma - 1} (-\overline{\rho} T' - \rho' \overline{T} + \rho' T' - \overline{\rho' T'}) - \frac{1}{2} (2\overline{\rho u'_k u'_k} + 2\overline{\rho' u'_k u'_k} + \rho' \overline{u_k u_k} + \right. \\ & \quad \left. 2\rho' \overline{u_k u'_k} + \rho' u'_k \overline{u'_k} + \overline{\rho u'_k u'_k} + 2\overline{u_k} \overline{\rho' u'_k} + \overline{\rho' u'_k u'_k}) \right]_{,t} = \\ & - \left\{ R_g (u'_{j,\overline{\rho} T} - \overline{u_j} \overline{\rho' T'} - u'_{j,\overline{\rho} T'} - \overline{u_j} \overline{\rho' T'} - u'_{j,\overline{\rho} T} - \overline{u_j} \overline{\rho' T'} + u'_{j,\overline{\rho} T} - \right. \\ & \quad \overline{\rho T'} u'_j - \overline{T} \rho' u'_j - \overline{u_j} \overline{\rho' T'} - \overline{\rho' T'} u'_j) + \frac{1}{2} (\overline{u_k} \overline{\rho u'_k u'_k} + \overline{u_k} \overline{\rho' u'_k u'_k} + 2\overline{u_k} \overline{\rho u'_k u'_k} + \\ & \quad u'_k \overline{\rho u'_k u'_k} + u'_k \overline{\rho' u'_k u'_k} + u'_k \overline{\rho u'_k u'_k} - \overline{u_k} \overline{\rho' u'_k u'_k} - \overline{u_k} \overline{\rho' u'_k u'_k} - 2u'_k \overline{\rho u'_k u'_k} - \\ & \quad u'_k \overline{\rho' u'_k u'_k} - u'_k \overline{\rho' u'_k u'_k} - \overline{\rho u'_k u'_k} - 2\overline{\rho u'_k u'_k} - 2\overline{u_j} \overline{u_k} \overline{\rho' u'_k} - \overline{u_k} \overline{u_k} \overline{\rho' u'_k} - \\ & \quad \overline{\rho u'_j u'_k} - \overline{u_j} \overline{\rho' u'_k} - 2\overline{u_k} \overline{\rho' u'_j} - \overline{\rho' u'_j u'_k}) + \kappa (T')_{,j} - \\ & \quad \left. \mu [u'_{i,j} \overline{u_i} + u'_{j,i} \overline{u_i} + \overline{u_i} u'_{j,i} + u'_{i,j} \overline{u'_i} + \overline{u_j} u'_{j,i} + u'_{j,i} \overline{u'_i} - 2\overline{u'_{j,i} u'_i} - \right. \\ & \quad \left. \frac{2}{3} (u'_{k,k} \overline{u_i} + \overline{u_{k,k}} u'_i + u'_{k,k} u'_i - \overline{u'_{i,j} u'_j}) \delta_{ij}] \right\}_{,j}. \end{aligned} \right. \tag{18}$$

We defined the function space $\mathcal{B}^{u'_N}$, $\mathcal{B}^{\rho'_N}$ and $\mathcal{B}^{T'_N}$, where the research problem is located, to satisfy the conditions as follows:

$$\left\{ \begin{aligned} & \mathcal{B}^{u'_N} = \left\{ [\xi^t_{ki}]_{k=1}^N \mid \xi^t_{ki} \in \mathcal{H}^N(\Omega), \int_{\Omega} \xi^t_{ki} \xi^t_{li} d\Omega = \delta_{kl}, \xi^t_{ki} \text{ second order differentiable} \right\}, \\ & \mathcal{B}^{\rho'_N} = \left\{ [\zeta^t_k]_{k=1}^N \mid \zeta^t_k \in \mathcal{H}^N(\Omega), \int_{\Omega} \zeta^t_k \zeta^t_{l} d\Omega = \delta_{kl}, \zeta^t_k \text{ second order differentiable} \right\}, \\ & \mathcal{B}^{T'_N} = \left\{ [\eta^t_k]_{k=1}^N \mid \eta^t_k \in \mathcal{H}^N(\Omega), \int_{\Omega} \eta^t_k \eta^t_l d\Omega = \delta_{kl}, \eta^t_k \text{ second order differentiable} \right\}. \end{aligned} \right. \tag{19}$$

We expressed u'_i , ρ' and T' as low-dimensional approximate forms in the function spaces $\mathcal{B}^{u'_N}$, $\mathcal{B}^{\rho'_N}$ and $\mathcal{B}^{T'_N}$, respectively, as follows. For convenience, the spatiotemporal optimal bases $\xi^t_{ki}, \zeta^t_k, \eta^t_k$ are expressed as $\xi_{ki}, \zeta_k, \eta_k$:

$$\left\{ \begin{aligned} & u'_i = a_k \xi_{ki} + u'_{Ri} \approx a_k \xi_{ki}, \\ & \rho' = b_k \zeta_k + \rho'_R \approx b_k \zeta_k, \\ & T' = c_k \eta_k + T'_R \approx c_k \eta_k, \end{aligned} \right. \tag{20}$$

where the truncation dimension N is omitted.

With spatiotemporal optimal bases $\xi_{ri}, \zeta_r, \eta_r$, the spectral expansion equation of the dimensional compressible turbulence middle-scale equation (18) is Galerkin formally projected onto unknown bases of $\xi_{ri}, \zeta_r, \eta_r$ respectively, to obtain the equation of the middle-scale dynamic system of compressible turbulence:

$$\left\{ \begin{aligned} & b_{r,t} = \mathcal{A}_r^I, \\ & a_{k,t} \mathcal{B}_{kr}^I + b_{l,t} \mathcal{B}_{lr}^II = \mathcal{B}_r^III, \\ & c_{m,t} \mathcal{C}_{mr}^I + b_{l,t} \mathcal{C}_{lr}^II + a_{k,t} \mathcal{C}_{kr}^III = \mathcal{C}_r^IV, \end{aligned} \right. \tag{21}$$

where the coefficients are as follows:

$$\mathcal{A}_r^I = \int_{\Omega} \overline{\rho' u'_{j,j} \zeta_r} d\Omega + \int_{\Omega} \overline{\rho' u'_{j,j} \zeta_r} d\Omega - \int_{\Omega} \overline{\rho u'_{j,j} \zeta_r} d\Omega - \int_{\Omega} \overline{\rho} u'_{j,j} \zeta_r d\Omega - \int_{\Omega} \rho' u'_{j,j} \zeta_r d\Omega - \int_{\Omega} \rho' u'_{j,j} \zeta_r d\Omega - \int_{\Omega} \rho' \overline{u_j} u'_{j,j} \zeta_r d\Omega - \int_{\Omega} \rho' \overline{u_j} u'_{j,j} \zeta_r d\Omega, \tag{22}$$

$$\mathcal{B}_{kr}^I = \int_{\Omega} \overline{\rho \xi_{ki} \xi_{ri}} d\Omega + \int_{\Omega} \rho' \xi_{ki} \xi_{ri} d\Omega - \int_{\Omega} \overline{\rho' \xi_{ki} \xi_{ri}} d\Omega, \tag{23}$$

$$\mathcal{B}_{lr}^{\text{II}} = \int_{\Omega} \bar{u}_i \zeta_l \xi_{ri} d\Omega + \int_{\Omega} \zeta_l u'_i \xi_{ri} d\Omega - \int_{\Omega} \overline{\zeta_l u'_i \xi_{ri}} d\Omega, \quad (24)$$

$$\begin{aligned} \mathcal{B}_{lr}^{\text{III}} = & - \int_{\Omega} \bar{\rho}_{,t} u'_i \xi_{ri} d\Omega - \int_{\Omega} \bar{u}_{i,t} \rho' \xi_{ri} d\Omega - \int_{\Omega} \bar{\rho}_{,j} \bar{u}_i u'_j \xi_{ri} d\Omega - \int_{\Omega} \bar{\rho} \bar{u}_{i,j} u'_j \xi_{ri} d\Omega - \int_{\Omega} \bar{\rho} \bar{u}_i u'_{j,j} \xi_{ri} d\Omega - \\ & \int_{\Omega} \bar{\rho}_{,j} u'_i \bar{u}_j \xi_{ri} d\Omega - \int_{\Omega} \bar{\rho} u'_{i,j} \bar{u}_j \xi_{ri} d\Omega - \int_{\Omega} \bar{\rho} u'_i \bar{u}_{j,j} \xi_{ri} d\Omega - \int_{\Omega} \bar{\rho}_{,j} u'_i u'_j \xi_{ri} d\Omega - \int_{\Omega} \bar{\rho} u'_{i,j} u'_j \xi_{ri} d\Omega - \\ & \int_{\Omega} \bar{\rho} u'_i u'_{j,j} \xi_{ri} d\Omega - \int_{\Omega} \rho' \bar{u}_i \bar{u}_j \xi_{ri} d\Omega - \int_{\Omega} \rho' \bar{u}_{i,j} \bar{u}_j \xi_{ri} d\Omega - \int_{\Omega} \rho' \bar{u}_i \bar{u}_{j,j} \xi_{ri} d\Omega - 2 \int_{\Omega} \rho' \bar{u}_i u'_j \xi_{ri} d\Omega - \\ & \int_{\Omega} \rho' \bar{u}_{i,j} u'_j \xi_{ri} d\Omega - \int_{\Omega} \rho' \bar{u}_i u'_{j,j} \xi_{ri} d\Omega - \int_{\Omega} \rho' u'_{i,j} \bar{u}_j \xi_{ri} d\Omega - \int_{\Omega} \rho' u'_i \bar{u}_{j,j} \xi_{ri} d\Omega - \int_{\Omega} \rho' u'_i u'_j \xi_{ri} d\Omega - \\ & \int_{\Omega} \rho' u'_{i,j} u'_j \xi_{ri} d\Omega - \int_{\Omega} \rho' u'_i u'_{j,j} \xi_{ri} d\Omega + \int_{\Omega} \bar{\rho}_{,j} \overline{u'_i u'_j \xi_{ri}} d\Omega + \int_{\Omega} \bar{\rho} \overline{u'_i u'_j \xi_{ri}} d\Omega + \int_{\Omega} \bar{\rho} \overline{u'_i u'_{j,j} \xi_{ri}} d\Omega + \\ & 2 \int_{\Omega} \bar{u}_{i,j} \overline{\rho' u'_j \xi_{ri}} d\Omega + 2 \int_{\Omega} \bar{u}_i \overline{\rho' u'_{j,j} \xi_{ri}} d\Omega + 2 \int_{\Omega} \bar{u}_i \overline{\rho' u'_i u'_j \xi_{ri}} d\Omega + \int_{\Omega} \bar{u}_{j,j} \overline{\rho' u'_i \xi_{ri}} d\Omega + \\ & \int_{\Omega} \bar{u}_j \overline{\rho' u'_i u'_j \xi_{ri}} d\Omega + \int_{\Omega} \bar{u}_j \overline{\rho' u'_{i,j} \xi_{ri}} d\Omega + \int_{\Omega} \rho' \overline{u'_i u'_j \xi_{ri}} d\Omega + \int_{\Omega} \rho' \overline{u'_i u'_{j,j} \xi_{ri}} d\Omega - \\ & R_g \delta_{ij} \left(\int_{\Omega} \bar{\rho}_{,j} T' \xi_{ri} d\Omega + \int_{\Omega} \bar{\rho} T'_{,j} \xi_{ri} d\Omega + \int_{\Omega} \rho'_{,j} \bar{T} \xi_{ri} d\Omega + \int_{\Omega} \rho' \bar{T}_{,j} \xi_{ri} d\Omega + \int_{\Omega} \rho'_{,j} T' \xi_{ri} d\Omega + \right. \\ & \left. \int_{\Omega} \rho' T'_{,j} \xi_{ri} d\Omega - \int_{\Omega} \overline{\rho'_{,j} T' \xi_{ri}} d\Omega - \int_{\Omega} \overline{\rho' T'_{,j} \xi_{ri}} d\Omega \right) + \mu \left(\int_{\Omega} u'_{i,j} \xi_{ri} d\Omega + \frac{1}{3} \int_{\Omega} u'_{j,i} \xi_{ri} d\Omega \right), \quad (25) \end{aligned}$$

$$C_{mr}^{\text{I}} = C_v \left(- \int_{\Omega} \bar{\rho} \eta_m \eta_r d\Omega + \int_{\Omega} \rho' \eta_m \eta_r d\Omega - \int_{\Omega} \overline{\rho' \eta_m \eta_r} d\Omega \right), \quad (26)$$

$$\begin{aligned} C_{lr}^{\text{II}} = & \left[C_v \left(- \int_{\Omega} \zeta_l \bar{T} \eta_r d\Omega + \int_{\Omega} \zeta_l T' \eta_r d\Omega - \int_{\Omega} \overline{\zeta_l T' \eta_r} d\Omega \right) - \right. \\ & \left. \frac{1}{2} \left(\int_{\Omega} \zeta_l \bar{u}_k \bar{u}_k \eta_r d\Omega + 2 \int_{\Omega} \zeta_l \bar{u}_k u'_k \eta_r d\Omega + \int_{\Omega} \zeta_l u'_k u'_k \eta_r d\Omega + \right. \right. \\ & \left. \left. 2 \int_{\Omega} \bar{u}_k \overline{\zeta_l u'_k \eta_r} d\Omega + \int_{\Omega} \overline{\zeta_l u'_k u'_k \eta_r} d\Omega \right) \right], \quad (27) \end{aligned}$$

$$\begin{aligned} C_{kr}^{\text{III}} = & - \left(\int_{\Omega} \bar{\rho} \bar{u}_i \xi_{kl} \eta_r d\Omega + 2 \int_{\Omega} \bar{\rho} \xi_{kl} u'_i \eta_r d\Omega + \int_{\Omega} \rho' \bar{u}_i \xi_{kl} \eta_r d\Omega + \right. \\ & \left. \int_{\Omega} \rho' \xi_{kl} u'_i \eta_r d\Omega + \int_{\Omega} \bar{\rho} \overline{\xi_{kl} u'_i \eta_r} d\Omega + \int_{\Omega} \bar{u}_i \overline{\rho' \xi_{kl} \eta_r} d\Omega + \int_{\Omega} \overline{\rho' \xi_{kl} u'_i \eta_r} d\Omega \right), \quad (28) \end{aligned}$$

$$\begin{aligned} C_r^{\text{IV}} = & - C_v \left(- \int_{\Omega} \bar{\rho}_{,t} T' \eta_r d\Omega - \int_{\Omega} \rho'_{,t} \bar{T} \eta_r d\Omega + \int_{\Omega} u'_{j,j} \bar{\rho} \bar{T} \eta_r d\Omega + \int_{\Omega} u'_j \bar{\rho}_{,j} \bar{T} \eta_r d\Omega + \right. \\ & \int_{\Omega} u'_j \bar{\rho} T'_{,j} \eta_r d\Omega - \int_{\Omega} \bar{u}_{j,j} \bar{\rho} T' \eta_r d\Omega - \int_{\Omega} \bar{u}_j \bar{\rho}_{,j} T' \eta_r d\Omega - \int_{\Omega} \bar{u}_j \bar{\rho} T'_{,j} \eta_r d\Omega - \\ & \int_{\Omega} u'_{j,j} \bar{\rho} T' \eta_r d\Omega - \int_{\Omega} u'_j \bar{\rho}_{,j} T' \eta_r d\Omega - \int_{\Omega} u'_j \bar{\rho} T'_{,j} \eta_r d\Omega - \int_{\Omega} \bar{u}_{j,j} \rho' \bar{T} \eta_r d\Omega - \\ & \int_{\Omega} \bar{u}_j \rho'_{,j} \bar{T} \eta_r d\Omega - \int_{\Omega} \bar{u}_j \rho' \bar{T}_{,j} \eta_r d\Omega - \int_{\Omega} u'_{j,j} \rho' \bar{T} \eta_r d\Omega - \int_{\Omega} u'_j T'_{,j} \bar{T} \eta_r d\Omega - \\ & \int_{\Omega} u'_j T' \bar{T}_{,j} \eta_r d\Omega + \int_{\Omega} \bar{u}_{j,j} \rho' T' \eta_r d\Omega + \int_{\Omega} \bar{u}_j \rho'_{,j} T' \eta_r d\Omega + \int_{\Omega} \bar{u}_j \rho' T'_{,j} \eta_r d\Omega + \\ & \int_{\Omega} u'_j \rho' T' \eta_r d\Omega + \int_{\Omega} u'_j \rho'_{,j} T' \eta_r d\Omega + \int_{\Omega} u'_j \rho' T'_{,j} \eta_r d\Omega - \int_{\Omega} \bar{\rho}_{,j} \overline{T' u'_j \eta_r} d\Omega - \\ & \int_{\Omega} \bar{\rho} \overline{T'_{,j} u'_j \eta_r} d\Omega - \int_{\Omega} \bar{\rho} \overline{T' u'_{j,j} \eta_r} d\Omega - \int_{\Omega} \bar{T}_{,j} \overline{\rho' u'_j \eta_r} d\Omega - \int_{\Omega} \bar{T} \overline{\rho'_{,j} u'_j \eta_r} d\Omega - \\ & \int_{\Omega} \bar{T} \overline{\rho' u'_{j,j} \eta_r} d\Omega - \int_{\Omega} \bar{u}_{j,j} \overline{\rho' T' \eta_r} d\Omega - \int_{\Omega} \bar{u}_j \overline{\rho'_{,j} T' \eta_r} d\Omega - \int_{\Omega} \bar{u}_j \overline{\rho' T'_{,j} \eta_r} d\Omega - \\ & \left. \int_{\Omega} \overline{\rho'_{,j} T' u'_j \eta_r} d\Omega - \int_{\Omega} \overline{\rho' T'_{,j} u'_j \eta_r} d\Omega - \int_{\Omega} \overline{\rho' T' u'_{j,j} \eta_r} d\Omega \right) - \\ & \frac{1}{2} \left(- 2 \int_{\Omega} \bar{\rho}_{,t} \bar{u}_k u'_k \eta_r d\Omega - 2 \int_{\Omega} \bar{\rho} \bar{u}_{k,t} u'_k \eta_r d\Omega - 2 \int_{\Omega} \bar{\rho}_{,t} u'_k u'_k \eta_r d\Omega - 2 \int_{\Omega} \rho' \bar{u}_{k,t} \bar{u}_k \eta_r d\Omega - \right. \end{aligned}$$

$$\begin{aligned}
& 2 \int_{\Omega} \rho' \overline{u_{k,t}} u'_k \eta_r d\Omega - \int_{\Omega} \overline{\rho'} u'_k \eta_r d\Omega - 2 \int_{\Omega} \overline{u_{k,t}} \rho' u'_k \eta_r d\Omega + 2 \int_{\Omega} \overline{u_{k,j}} \overline{\rho} u'_k \eta_r d\Omega + \\
& \int_{\Omega} \overline{u_k} \overline{\rho_j} \overline{u_k} u'_k \eta_r d\Omega + \int_{\Omega} \overline{u_{k,j}} \overline{\rho} u'_k \overline{u_j} \eta_r d\Omega + \int_{\Omega} \overline{u_k} \overline{\rho_j} u'_k \overline{u_j} \eta_r d\Omega + \int_{\Omega} \overline{u_k} \overline{\rho} u'_k \overline{u_{j,j}} \eta_r d\Omega + \\
& 2 \int_{\Omega} \overline{u_{k,j}} \overline{\rho} u'_k u'_j \eta_r d\Omega + 2 \int_{\Omega} \overline{u_k} \overline{\rho_j} u'_k u'_j \eta_r d\Omega + 2 \int_{\Omega} \overline{u_k} \overline{\rho} u'_k u'_j \eta_r d\Omega + 2 \int_{\Omega} \overline{u_k} \overline{\rho} u'_k u'_{j,j} \eta_r d\Omega + \\
& \int_{\Omega} u'_k \overline{\rho_j} \overline{u_k} \overline{u_j} \eta_r d\Omega + \int_{\Omega} u'_k \overline{\rho} \overline{u_{k,j}} \overline{u_j} \eta_r d\Omega + \int_{\Omega} u'_k \overline{\rho} \overline{u_k} \overline{u_{j,j}} \eta_r d\Omega + \int_{\Omega} u'_k \overline{\rho_j} u'_k \overline{u_j} \eta_r d\Omega + \\
& 2 \int_{\Omega} u'_k \overline{\rho} u'_{k,j} \overline{u_j} \eta_r d\Omega + \int_{\Omega} u'_k \overline{\rho} u'_{k,j} \overline{u_{j,j}} \eta_r d\Omega + 2 \int_{\Omega} u'_{k,j} \overline{\rho} u'_k u'_j \eta_r d\Omega + \\
& \int_{\Omega} u'_k \overline{\rho_j} u'_k u'_j \eta_r d\Omega + \int_{\Omega} u'_k \overline{\rho} u'_k u'_{j,j} \eta_r d\Omega - 2 \int_{\Omega} \overline{u_{k,j}} \rho' \overline{u_k} \overline{u_j} \eta_r d\Omega - \int_{\Omega} \overline{u_k} \rho'_j \overline{u_k} \overline{u_j} \eta_r d\Omega - \\
& \int_{\Omega} \overline{u_k} \rho' \overline{u_k} \overline{u_{j,j}} \eta_r d\Omega - 2 \int_{\Omega} \overline{u_{k,j}} \rho' \overline{u_k} u'_j \eta_r d\Omega - \int_{\Omega} \overline{u_k} \rho'_j \overline{u_k} u'_j \eta_r d\Omega - \\
& \int_{\Omega} \overline{u_k} \rho' \overline{u_k} u'_{j,j} \eta_r d\Omega - 2 \int_{\Omega} u'_{k,j} \rho' \overline{u_k} \overline{u_j} \eta_r d\Omega - 2 \int_{\Omega} u'_k \rho'_j \overline{u_k} \overline{u_j} \eta_r d\Omega - \\
& 2 \int_{\Omega} u'_k \rho' \overline{u_{k,j}} \overline{u_j} \eta_r d\Omega - 2 \int_{\Omega} u'_k \rho' \overline{u_k} \overline{u_{j,j}} \eta_r d\Omega - \int_{\Omega} u'_{k,j} \rho' u'_k \overline{u_j} \eta_r d\Omega - \int_{\Omega} u'_k \rho'_j u'_k \overline{u_j} \eta_r d\Omega - \\
& \int_{\Omega} u'_k \rho' u'_{k,j} \overline{u_j} \eta_r d\Omega - \int_{\Omega} u'_k \rho' u'_k \overline{u_{j,j}} \eta_r d\Omega - 2 \int_{\Omega} u'_{k,j} \rho' u'_k u'_j \eta_r d\Omega - \int_{\Omega} u'_k \rho'_j u'_k u'_j \eta_r d\Omega - \\
& \int_{\Omega} u'_k \rho' u'_k u'_{j,j} \eta_r d\Omega - \int_{\Omega} \overline{\rho_j} \overline{u_j} \overline{u'_k} \overline{u'_k} \eta_r d\Omega - \int_{\Omega} \overline{\rho} \overline{u_{j,j}} \overline{u'_k} \overline{u'_k} \eta_r d\Omega - 2 \int_{\Omega} \overline{\rho} \overline{u_j} \overline{u'_{k,j}} \overline{u'_k} \eta_r d\Omega - \\
& 2 \int_{\Omega} \overline{\rho_j} \overline{u_k} \overline{u'_j} \overline{u'_k} \eta_r d\Omega - 2 \int_{\Omega} \overline{\rho} \overline{u_{k,j}} \overline{u'_j} \overline{u'_k} \eta_r d\Omega - 2 \int_{\Omega} \overline{\rho} \overline{u_k} \overline{u'_{j,j}} \overline{u'_k} \eta_r d\Omega - 2 \int_{\Omega} \overline{\rho} \overline{u_k} \overline{u'_j} \overline{u'_k} \eta_r d\Omega - \\
& 2 \int_{\Omega} \overline{u_{j,j}} \overline{u_k} \overline{\rho'} \overline{u'_k} \eta_r d\Omega - 2 \int_{\Omega} \overline{u_j} \overline{u_{k,j}} \overline{\rho'} \overline{u'_k} \eta_r d\Omega - 2 \int_{\Omega} \overline{u_j} \overline{u_k} \overline{\rho'_j} \overline{u'_k} \eta_r d\Omega - 2 \int_{\Omega} \overline{u_j} \overline{u_k} \overline{\rho'} \overline{u'_{k,j}} \eta_r d\Omega - \\
& 2 \int_{\Omega} \overline{u_{k,j}} \overline{u_k} \overline{\rho'} u'_j \eta_r d\Omega - \int_{\Omega} \overline{u_k} \overline{u_k} \overline{\rho'_j} u'_j \eta_r d\Omega - \int_{\Omega} \overline{u_k} \overline{u_k} \overline{\rho'} u'_{j,j} \eta_r d\Omega - \int_{\Omega} \overline{\rho_j} \overline{u'_j} u'_k \overline{u'_k} \eta_r d\Omega - \\
& \int_{\Omega} \overline{\rho} \overline{u'_{j,j}} u'_k \overline{u'_k} \eta_r d\Omega - 2 \int_{\Omega} \overline{\rho} \overline{u'_j} u'_{k,j} \overline{u'_k} \eta_r d\Omega - \int_{\Omega} \overline{u_{j,j}} \overline{\rho'} u'_k \overline{u'_k} \eta_r d\Omega - \int_{\Omega} \overline{u_j} \overline{\rho'_j} u'_k \overline{u'_k} \eta_r d\Omega - \\
& 2 \int_{\Omega} \overline{u_j} \overline{\rho'} u'_{k,j} \overline{u'_k} \eta_r d\Omega - 2 \int_{\Omega} \overline{u_{k,j}} \overline{\rho'} u'_j \overline{u'_k} \eta_r d\Omega - 2 \int_{\Omega} \overline{u_k} \overline{\rho'_j} u'_j \overline{u'_k} \eta_r d\Omega - 2 \int_{\Omega} \overline{u_k} \overline{\rho'} u'_{j,j} \overline{u'_k} \eta_r d\Omega - \\
& 2 \int_{\Omega} \overline{u_k} \overline{\rho'} u'_j \overline{u'_{k,j}} \eta_r d\Omega - \int_{\Omega} \overline{\rho'_j} u'_j u'_k \overline{u'_k} \eta_r d\Omega - \int_{\Omega} \overline{\rho'} u'_{j,j} u'_k \overline{u'_k} \eta_r d\Omega - 2 \int_{\Omega} \overline{\rho'} u'_j u'_{k,j} \overline{u'_k} \eta_r d\Omega \Big) - \\
& \kappa \int_{\Omega} T'_{j,j} \eta_r d\Omega + \mu \left[\int_{\Omega} u'_{i,jj} \overline{u_i} \eta_r d\Omega + \int_{\Omega} u'_{i,j} \overline{u_{i,j}} \eta_r d\Omega + \int_{\Omega} u'_{j,ij} \overline{u_i} \eta_r d\Omega + \int_{\Omega} u'_{j,i} \overline{u_{i,j}} \eta_r d\Omega + \right. \\
& \int_{\Omega} \overline{u_{i,jj}} u'_i \eta_r d\Omega + \int_{\Omega} \overline{u_{i,j}} u'_{i,j} \eta_r d\Omega + \int_{\Omega} u'_{i,jj} u'_i \eta_r d\Omega + \int_{\Omega} u'_{i,j} u'_{i,j} \eta_r d\Omega + \int_{\Omega} \overline{u_{j,ij}} u'_i \eta_r d\Omega + \\
& \int_{\Omega} \overline{u_{j,i}} u'_{i,j} \eta_r d\Omega + \int_{\Omega} u'_{j,ij} u'_i \eta_r d\Omega + \int_{\Omega} u'_{j,i} u'_{i,j} \eta_r d\Omega - 2 \int_{\Omega} \overline{u'_{j,ij}} u'_i \eta_r d\Omega - \\
& \left. 2 \int_{\Omega} \overline{u'_{j,i}} u'_{i,j} \eta_r d\Omega - \frac{2}{3} \left(\int_{\Omega} u'_{k,kj} \overline{u_i} \delta_{ij} \eta_r d\Omega + 2 \int_{\Omega} u'_{k,k} \overline{u_{i,j}} \delta_{ij} \eta_r d\Omega + \int_{\Omega} \overline{u_{k,kj}} u'_i \delta_{ij} \eta_r d\Omega + \right. \right. \\
& \left. \left. \int_{\Omega} u'_{k,kj} u'_i \delta_{ij} \eta_r d\Omega + \int_{\Omega} u'_{k,k} u'_{i,j} \delta_{ij} \eta_r d\Omega - \int_{\Omega} \overline{u'_{i,jj}} u'_j \delta_{ij} \eta_r d\Omega - \int_{\Omega} \overline{u'_{i,j} u'_{j,i}} \delta_{ij} \eta_r d\Omega \right) \right]. \quad (29)
\end{aligned}$$

6.2.3 Optimal Functional of Middle-Scale Dynamical System J

The optimal functional for approximating the initial conditions of a dimensional compressible turbulence middle-scale dynamical system J can be found below.

With middle-scale optimal bases for approximating the initial conditions of large-scale fields ξ_{ki} , ζ_k , η_k , the following optimal functional can be obtained:

$$\left\{ \begin{aligned}
 J(\xi_{ki}, \zeta_k, \eta_k) &= \int_{\Omega} (\overline{u_{Ri}(0)}, \overline{u_{Ri}(0)}) \, d\Omega + \int_{\Omega} (\overline{\rho_R(0)}, \overline{\rho_R(0)}) \, d\Omega + \int_{\Omega} (\overline{T_R(0)}, \overline{T_R(0)}) \, d\Omega = \\
 &\int_{\Omega} \left(\overline{u_i(0)} - a_k(0)\xi_{ki} \right) \left(\overline{u_i(0)} - a_k(0)\xi_{ki} \right) \, d\Omega + \\
 &\int_{\Omega} \left(\overline{\rho(0)} - b_k(0)\zeta_k \right) \left(\overline{\rho(0)} - b_k(0)\zeta_k \right) \, d\Omega + \\
 &\int_{\Omega} \left(\overline{T(0)} - c_k(0)\eta_k \right) \left(\overline{T(0)} - c_k(0)\eta_k \right) \, d\Omega = \\
 &\int_{\Omega} \left[\overline{u_i(0)} \overline{u_i(0)} - 2a_k(0)\xi_{ki}\overline{u_i(0)} + a_k(0)\xi_{ki}a_k(0)\xi_{ki} \right] \, d\Omega + \\
 &\int_{\Omega} \left[\overline{\rho(0)} \overline{\rho(0)} - 2b_k(0)\zeta_k\overline{\rho(0)} + b_k(0)\zeta_k b_k(0)\zeta_k \right] \, d\Omega + \\
 &\int_{\Omega} \left[\overline{T(0)} \overline{T(0)} - 2c_k(0)\eta_k\overline{T(0)} + c_k(0)\eta_k c_k(0)\eta_k \right] \, d\Omega,
 \end{aligned} \right. \quad (30)$$

where $\overline{u_i(0)}$, $\overline{\rho(0)}$, $\overline{T(0)}$ are the initial values of the known large-scale field.

6.2.4 Solution Procedure of the LMS Method

At the initial moment, the concept of the turbulence intensity^[10-11] is adopted:

$$I \equiv \frac{u'}{U} = 0.16Re^{-\frac{1}{8}}. \quad (31)$$

The initial values of the middle-scale flow field variables $u_i(0)$, $\rho(0)$, $T(0)$ are obtained, where $U = \sqrt{\overline{u_i} \overline{u_i}}$ is the large-scale velocity and Re is the Reynolds number,

With the scale similarity concept, the large-scale POD bases of ξ_{ki}^0 , ζ_k^0 , η_k^0 and the large-scale flow field in a large-scale grid are interpolated into a middle-scale grid ($\Delta x/2^p$, $p \geq 1$), and the large-scale POD bases are used as the initial middle-scale bases to obtain the initial condition of their coefficients:

$$\begin{cases}
 b_k(0) = (\rho(0), \zeta_k), \\
 a_k(0) = (u_i(0), \xi_{ki}), \\
 c_k(0) = (T(0), \eta_k).
 \end{cases} \quad (32)$$

The fourth-order Runge-Kutta method and ill-conditioned AFD algorithm are used to solve the middle-scale optimal low-dimensional dynamical system equation (21) to obtain a_k^i, b_k^i, c_k^i ;

♣ We used equation (20) to obtain the new solution of the middle-scale flow field and the correlation functions (14), and the small-scale SGS terms equations (15), (16) and (17);

Using the middle-scale flow field variables and the correlation functions, which are on the overlapped large- and middle-scale grids and the small-scale SGS terms equations (15), (16) and (17), to obtain the terms on the right-hand side of equation (13), the new solution of the large-scale flow field can be obtained by substituting these into the large-scale equation (13), and the new solution of the large-scale flow field is applied to the middle-scale dynamical system equation (21).

We used equation (30) together with the new values of the large-scale flow field interpolated into the middle-scale grid to obtain the new spatiotemporal optimal bases $\xi_{ki}, \zeta_k, \eta_k$.

Goto ♣ or the LMS simulation is completed.

In this way, the approximate solution of the turbulence flow field (= large-scale mean field+middle-scale flow field) can also be obtained.

6.3 Numerical Simulation of the Re-Shock Richtmyer-Meshkov Instability Problem With the LMS Method

6.3.1 Problem Description

The initial state of the re-shock RM instability problem is shown in [fig. 4](#).

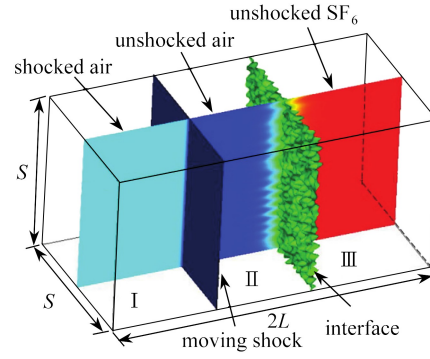


Fig. 4 Schematic diagram of the re-shock RMI initial state in a rectangular cavity

The re-shock RM instability of light/heavy fluid interfaces with multimodal initial disturbances under plane shock acceleration in the shock tube is studied.

$$D = \{\mathbf{x} | 0 \leq y, z \leq S, 0 \leq x \leq 2L\}, \quad (33)$$

where $S = 0.01$ m and $L = 0.014$ m. The numbers of equal spacing grids are flow direction grids \times spanwise grids \times normal grid = $147 \times 61 \times 61 = 546\,987$. The time step is $0.000\,000\,1$ s. The shock wave initially located at $x = 0.01$ m moves in the x direction, and the shock Mach number is $Ma_S = 1.5$. The initial interface is located at $x = L$, and the initial interface function is

$$\varphi(\mathbf{x}) = x - L - \eta(y, z) = 0. \quad (34)$$

We adopted the multimodal perturbation form provided by Tritschler et al.^[12]

$$\eta(y, z) = a_0 \sum_{n=1}^{13} \sum_{m=3}^{15} a_{n,m} \sin(k_n y + \phi_n) \sin(k_m z + \chi_m), \quad (35)$$

where the main amplitude is $a_0 = 4 \times 10^{-5}$ m, the secondary amplitudes of different modes are $a_{n,m} = \sin(nm)/2$, the wave numbers are $k_n = 2\pi n/L$ and $k_m = 2\pi m/L$, and the phase shifts are $\phi_n = \tan(n)$ and $\chi_n = \tan(m)$. Although equation (35) is similar to the form of random perturbation, it has a definite expression and can be repeatedly constructed in different examples.

The light/heavy fluids on both sides of the interface are composed of air/SF₆ components, and their molar masses are $M_1 = 28.964$ g \cdot mol⁻¹ and $M_2 = 146.057$ g \cdot mol⁻¹, respectively. We set the initial pressure and temperature to $p_0 = 23\,000$ Pa and $T_0 = 298$ K, respectively. Then, the density is obtained from the equation of state (10):

$$\rho_i = \frac{p_0 M_i}{RT_0}, \quad (36)$$

i.e.,

$$\rho_1 = \frac{p_0 M_1}{RT_0} = \frac{23\,000 \text{ Pa} \times 28.964 \text{ g} \cdot \text{mol}^{-1}}{8.314 \text{ Pa} \cdot \text{m}^3 \cdot \text{K}^{-1} \times 298 \text{ K}} = 0.269 \text{ kg/m}^3, \quad (37)$$

$$\rho_2 = \frac{p_0 M_2}{RT_0} = \frac{23\,000 \text{ Pa} \times 146.057 \text{ g} \cdot \text{mol}^{-1}}{8.314 \text{ Pa} \cdot \text{m}^3 \cdot \text{K}^{-1} \times 298 \text{ K}} = 1.356 \text{ kg/m}^3. \quad (38)$$

Atwood number is

$$A = \frac{\rho_2 - \rho_1}{\rho_1 + \rho_2} = \frac{1.356 - 0.269}{0.269 + 1.356} = 0.669. \quad (39)$$

6.3.2 Initial and Boundary Conditions

1) Initial condition

In summary, it can be seen that in the study of RM instability, the fluid inside the shock tube at the initial moment is divided into three regions by the shock wave and interface: light fluid behind the wave (zone I), light fluid before the wave (zone II), and heavy fluid before the wave (zone III). The light fluid after the shock wave

needs to be determined on the shock wave, before and after, by the Rankine Hugoniot condition^[13], and the specific heat ratio is $\gamma_1 = 1.4$. The specific expression of the density is as follows:

$$\rho_S = \frac{(\gamma_1 + 1)Ma_S^2}{2 + (\gamma_1 - 1)Ma_S^2} \rho_1 = \frac{(1.4 + 1) \times 1.5^2}{2 + (1.4 - 1) \times 1.5^2} \times 0.269 = 0.501 \text{ kg/m}^3. \quad (40)$$

The pressure can be expressed as follows:

$$p_S = \frac{2\gamma_1 Ma_S^2 - \gamma_1 + 1}{\gamma_1 + 1} p_0 = \frac{2 \times 1.4 \times 1.5^2 - 1.4 + 1}{1.4 + 1} \times 23\,000 = 56\,541.667 \text{ Pa}. \quad (41)$$

Finally, the velocity can be represented as follows:

$$U_S = U_S \mathbf{i}, \quad U_S = \frac{2(Ma_S^2 - 1)}{(\gamma_1 + 1)Ma_S} \sqrt{\frac{\gamma_1 p_0}{\rho_1}} = \frac{2 \times (1.5^2 - 1)}{(1.4 + 1) \times 1.5} \sqrt{\frac{1.4 \times 23\,000}{0.269}} = 240.26 \text{ m/s}. \quad (42)$$

The temperature is also determined by the equation of state (10) as follows:

$$T_S = \frac{p_S M_1}{\rho_S R} = \frac{56\,541.667 \times 28.964}{0.501 \times 8.314} = 393\,169.121 \text{ K}. \quad (43)$$

Therefore, the initial conditions for the RM instability problems can be summarized as follows:

$$\begin{aligned} \rho(\mathbf{x}, t = 0) &= (\rho_2 - \rho_1)H(\varphi) - (\rho_S - \rho_1)H\left(\frac{x-L}{L} + \frac{1}{2}\right) + \rho_S = \\ &= (1.356 - 0.269)H(x - 0.01 - \eta(y, z)) - (0.501 - 0.269)H\left(\frac{x-0.01}{0.01} + 0.5\right) + 0.501 = \\ &= 0.5435 \left[\text{erf}\left(\frac{x-0.01-\eta(y,z)}{2\delta_0}\right) + 1 \right] - 0.116 \left[\text{erf}\left(\frac{100x-0.5}{2\delta_0}\right) + 1 \right] + 0.501 \text{ kg/m}^3, \end{aligned} \quad (44)$$

$$\begin{aligned} \mathbf{u}(\mathbf{x}, t = 0) &= \left[1 - H\left(\frac{x-L}{L} + \frac{1}{2}\right) \right] U_S \mathbf{i} = \left[1 - H\left(\frac{x-0.01}{0.01} + 0.5\right) \right] 240.26 \mathbf{i} = \\ &= \left\{ 1 - 0.5 \left[\text{erf}\left(\frac{100x-0.5}{2\delta_0}\right) + 1 \right] \right\} 240.26 \mathbf{i} \text{ m/s}, \end{aligned} \quad (45)$$

$$\begin{aligned} p(\mathbf{x}, t = 0) &= -(p_S - p_0)H\left(\frac{x-L}{L} + \frac{1}{2}\right) + p_S = \\ &= -(56\,541.667 - 23\,000)H\left(\frac{x-0.01}{0.01} + 0.5\right) + 56\,541.667 \\ &= -16\,770.8335 \left[\text{erf}\left(\frac{100x-0.5}{2\delta_0}\right) + 1 \right] + 56\,541.667 \text{ Pa}, \end{aligned} \quad (46)$$

$$\begin{aligned} T(\mathbf{x}, t = 0) &= -(T_S - T_0)H\left(\frac{x-L}{L} + \frac{1}{2}\right) + T_S = \\ &= -(393\,169.121 - 298)H\left(\frac{x-0.01}{0.01} + 0.5\right) + 393\,169.121 = \\ &= -196\,435.5605 \left[\text{erf}\left(\frac{100x-0.5}{2\delta_0}\right) + 1 \right] + 393\,169.121 \text{ K}, \end{aligned} \quad (47)$$

where H is the Heaviside function

$$H = \begin{cases} 0, & t < 0, \\ 1, & t \leq 0. \end{cases} \quad (48)$$

We used the error function to perform the following smoothing operations:

$$H = \frac{1}{2} \left[\text{erf}\left(\frac{\alpha}{2\delta_0}\right) + 1 \right]. \quad (49)$$

Its thickness can be set to a grid scale of $\delta_0 = \Delta x$. Meanwhile, due to the acceleration of the shock wave at the interface, it will generate an x directional translation velocity of $U_0^+ = 158.1 \text{ m} \cdot \text{s}^{-1}$. Therefore, to maintain the

interface in the initial position during the calculation process, the initial velocity in the direction of (45) should be subtracted from U_0^+ .

2) Boundary condition

The RM instability satisfies the periodic boundary conditions in the y and z directions, and the boundaries in the x direction are non-slip solid walls.

6.3.3 Numerical Results of the Re-Shock Richtmyer-Meshkov Instability

The parameters used in the following numerical results of the re-shock Richtmyer-Meshkov instability are the dimensions of the spatiotemporal multiscale optimal low-dimensional dynamical system of the middle-scale equation $N = 3$, Reynolds number $Re = 3\,608\,549$, Mach number $Ma = 0.6$, Prandtl number $Pr = 0.72$ and simulation time $t = 0 \sim 0.0024$ s. In following figures, the upper, middle and lower figures show the iso-surface of middle-scale fields (ρ' , T' , u' , v' , w'), the large-scale mean fields ($\bar{\rho}$, \bar{T} , \bar{u} , \bar{v} , \bar{w}), and the approximate solutions of turbulence (ρ , T , u , v , w), respectively.

From [figs. 5 to 9](#), it can be seen that the RM instability interface is repeatedly rubbed by the re-shock wave to produce a large amount of smaller flow structures close to the middle part in the middle-scale and large-scale flow fields and to obtain another kind of very interesting approximate solution of turbulence other than that of DNS for the first time.

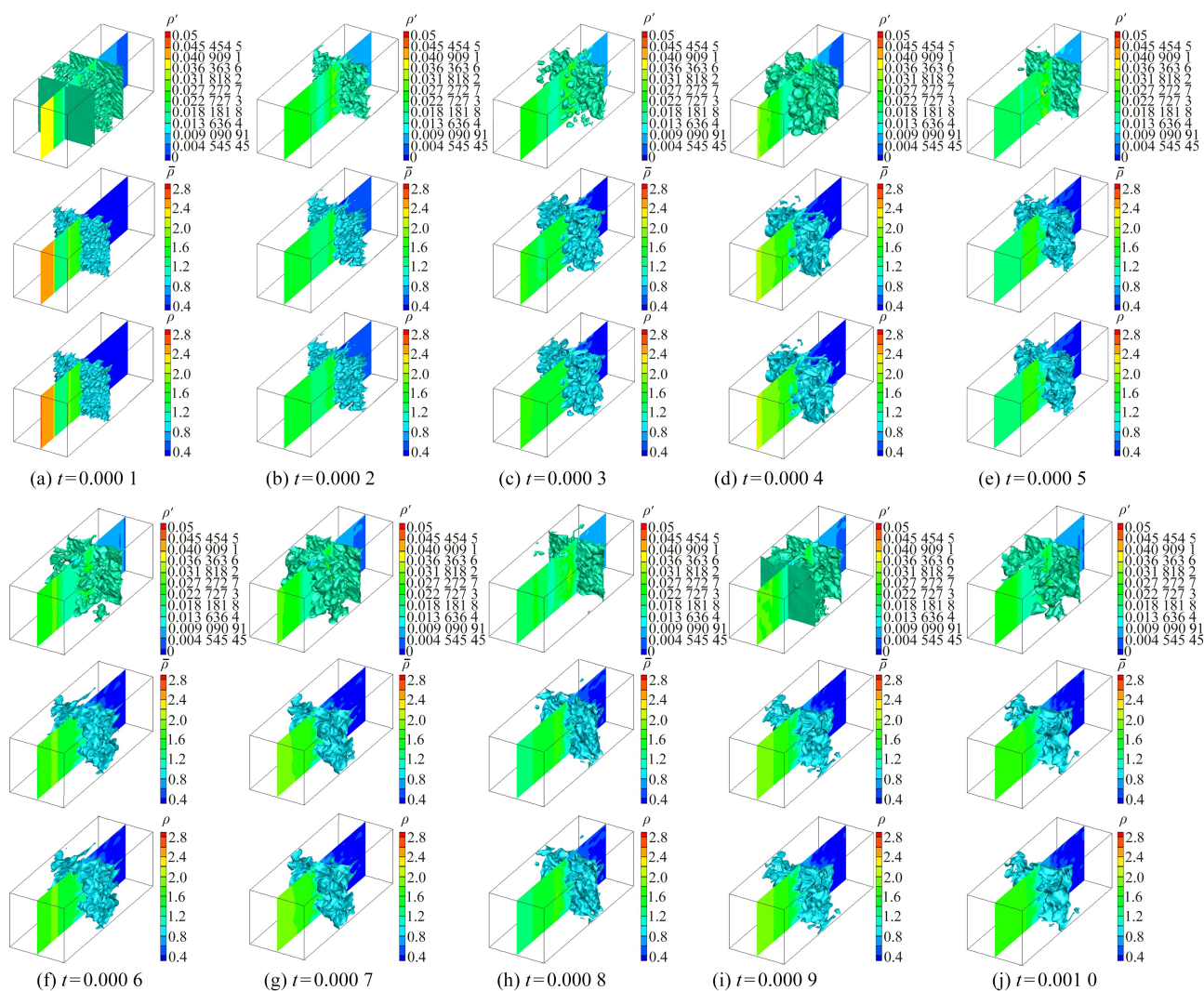


Fig. 5 Time evolution of iso-surface of ρ of the re-shock RM

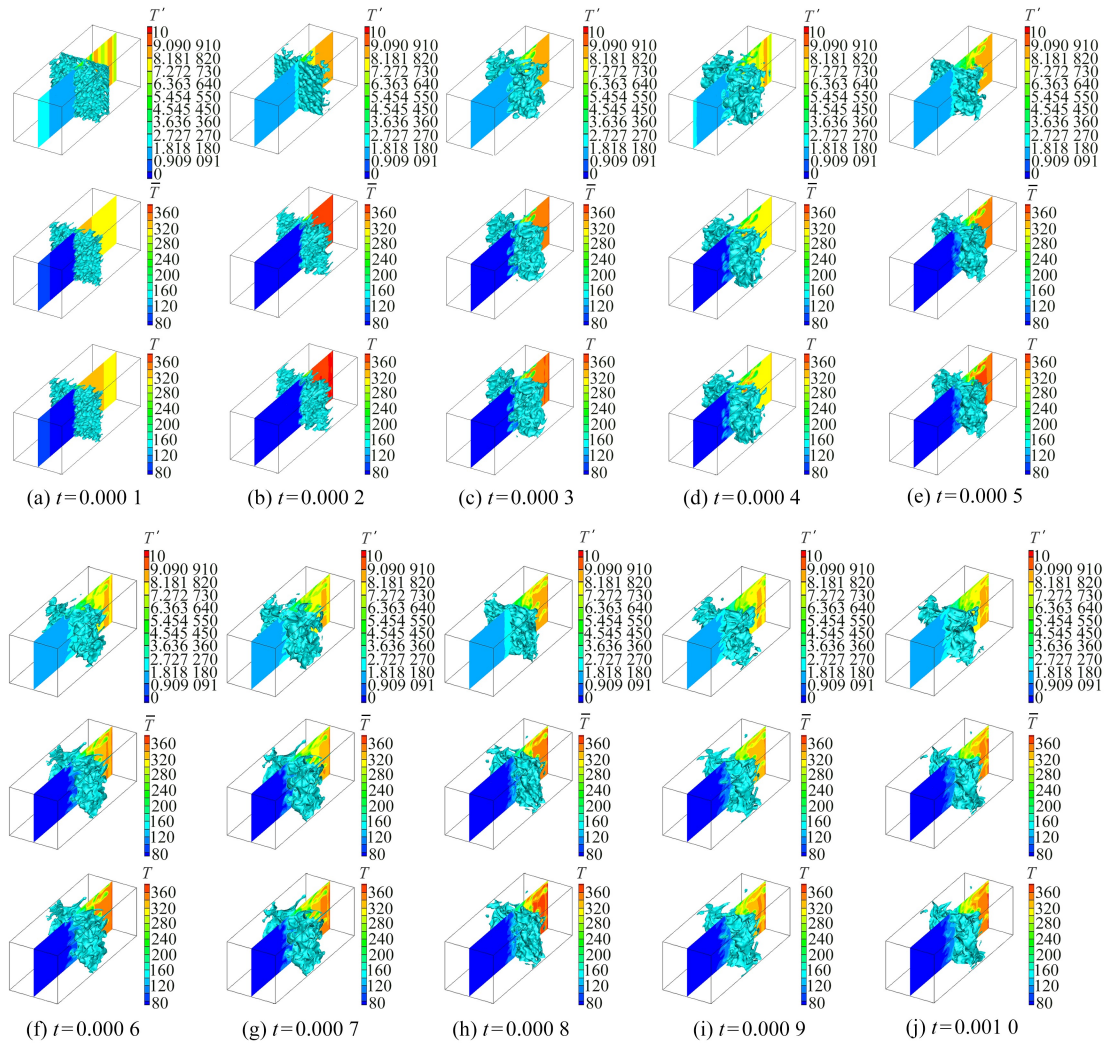
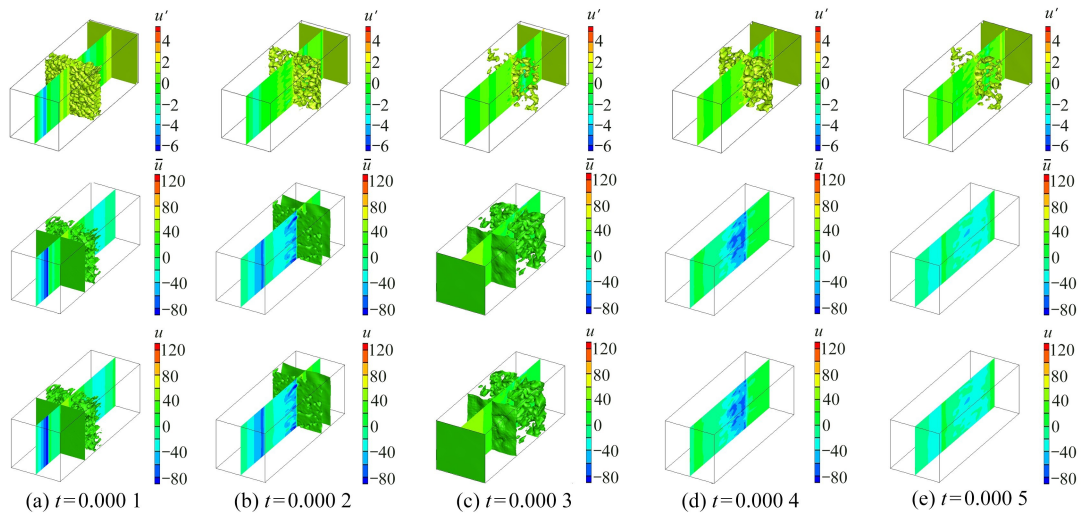


Fig. 6 Time evolution of iso-surface of T of the re-shock RM

Because the purpose of this paper is to point out that there are a few big problems in the theoretical basis of turbulence modeling, and then setup a new and multi-scale numerical simulation method for compressible turbulence (LMS), therefore there is no need to conduct a careful physical analysis of the results.



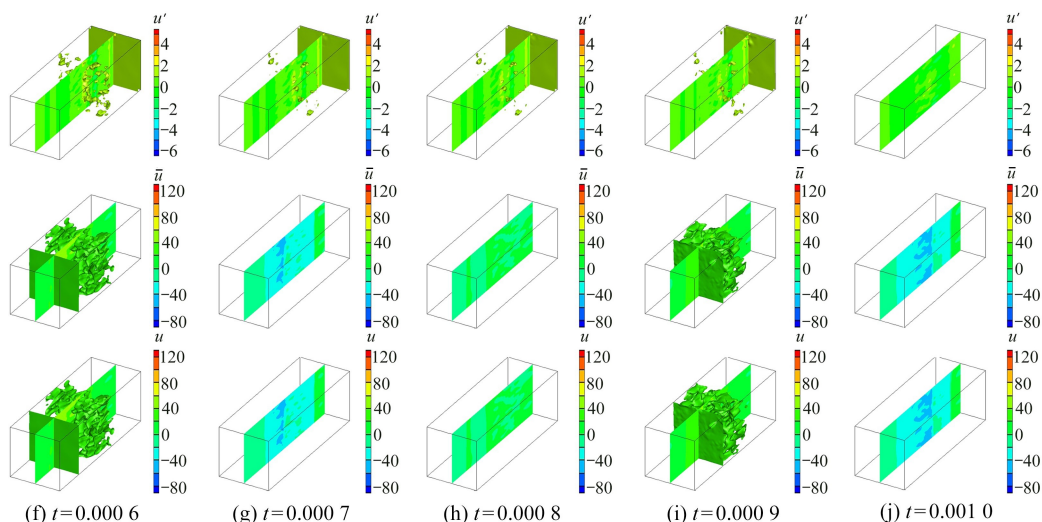


Fig. 7 Time evolution of iso-surface of u of the re-shock RM

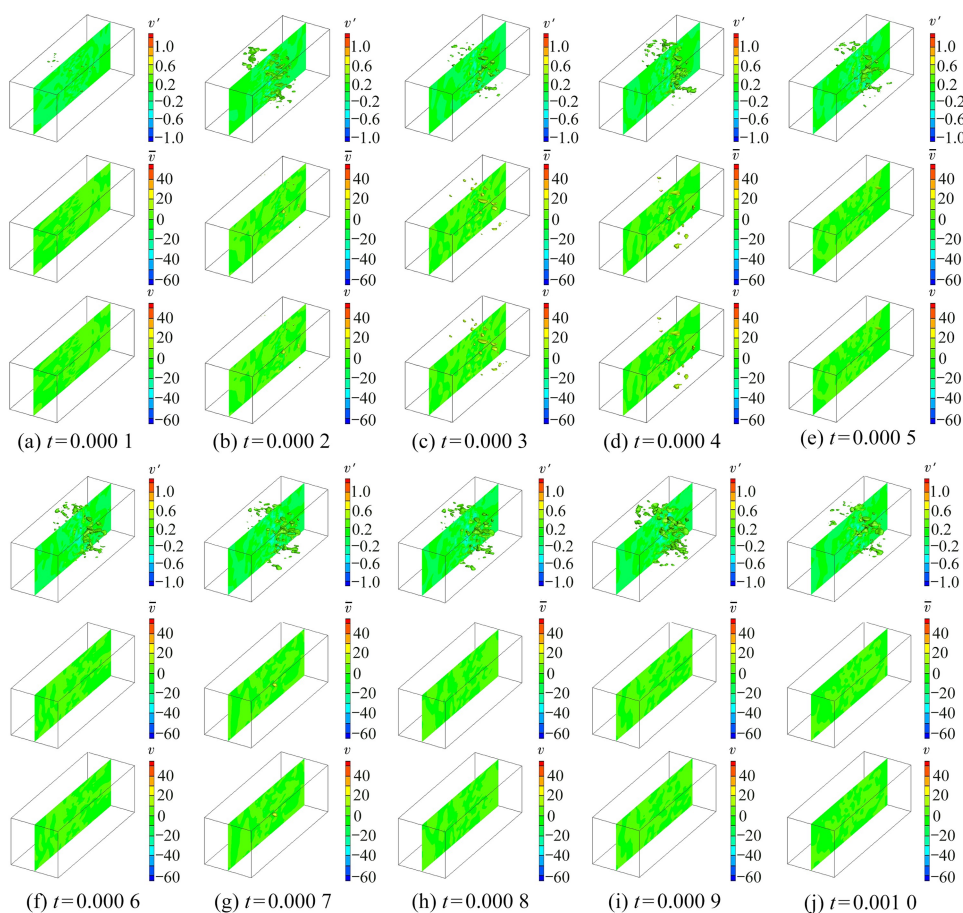


Fig. 8 Time evolution of iso-surface of v of the re-shock RM

Since the LMS method is a new independent numerical simulation method of turbulence based on first principles and without any artificial assumptions, its theoretical basis is consistent; therefore, it is not necessary to verify its correctness through quantitative comparison with DNS coarse-grained results.

It must be noted that it is wrong to directly compare the numerical results of the RANS, LES, DES or LMS with those of the DNS. The correct method is to first coarse-grain the DNS numerical results on the RANS, LES, DES or LMS grid and then compare their results quantitatively.

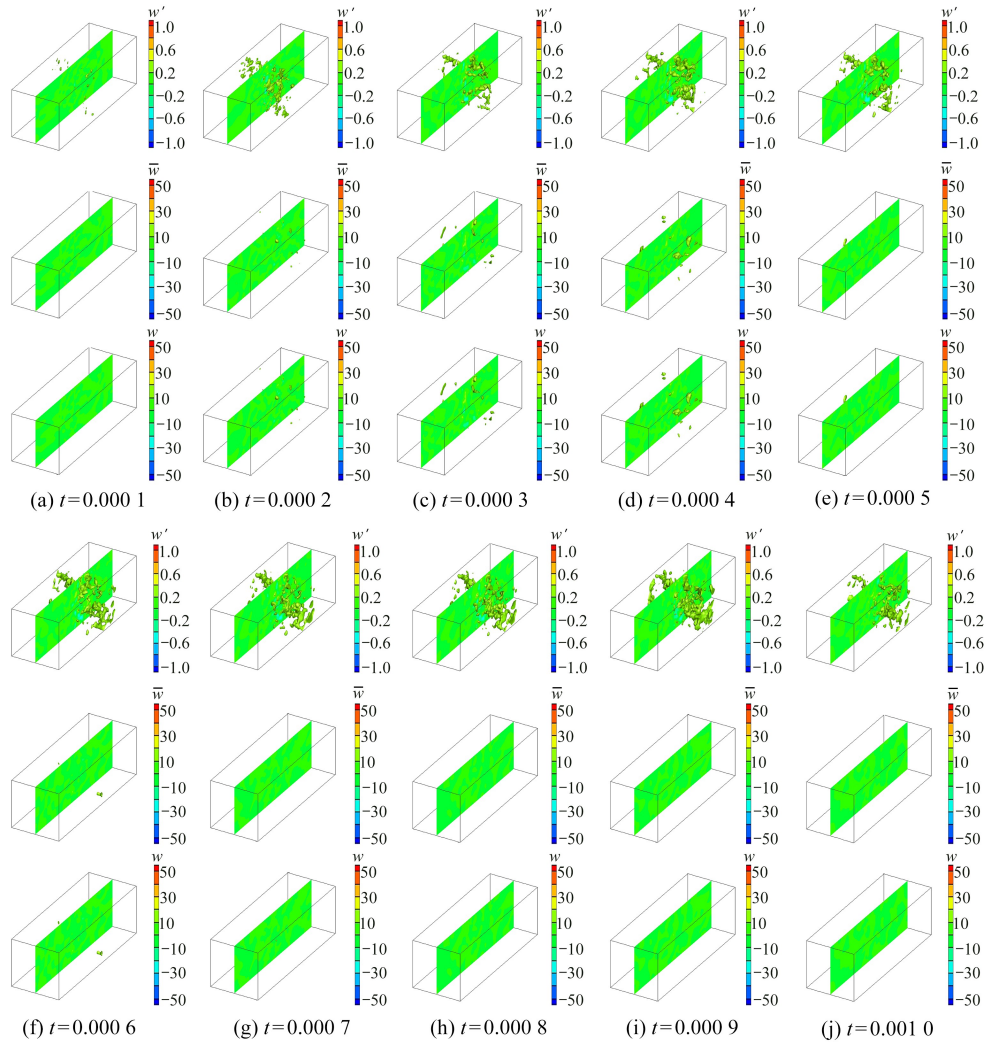


Fig. 9 Time evolution of iso-surface of w of the re-shock RM

7 Conclusions

According to Professor P-Y CHOU's idea^[2] in which “the turbulence should be studied by analyzing and solving the fluctuating velocity field”, we revisit the theoretical bases of turbulence modeling before setting up the LMS method and examined the following aspects.

Based on the physical characteristics of turbulence, a new concept of large-, middle- and small-scale decompositions of turbulence is proposed. The relationship between the correlation function and filtering (averaging) function is analyzed, and the algorithm for the correlation function is clarified. A long-standing logical error in the theory of turbulence models is pointed out, and the correct theoretical basis of the numerical simulation of turbulence and the concept of a multiscale turbulence model are given. The philosophical essence is indicated, and an iterative multiscale method is successfully employed to overcome the closure problem of turbulence. The errors in the quantitative comparison of turbulence numerical simulation results are studied, and a coarse-grained quantitative comparison method is provided.

Then, the LMS method is systematically established, and the turbulent middle-scale flow field and the spatiotemporally accurate solution of turbulence are obtained with the LES grid, which deepens the understanding of the complexity of turbulence. The multiscale characteristics of turbulence are naturally included in the middle- and small-scale modeling, there is no logic error in the LMS method, and the approximate solution of turbulence f can

be obtained. Due to the use of first principles in the LMS method, the LMS method is suitable for the numerical simulation of various complex turbulent flows, and fewer grid points can be used in the LMS method to obtain a more accurate solution of turbulence. With the box filtering, the space grid average, and in the sense of a large-scale grid, the essence of the LMS method is a turbulence numerical simulation method that integrates the RANS, LES, DES and DNS.

Finally, it is necessary to indicate that the LMS method can also be served as an auxiliary tool for turbulence model research to examine whether the turbulence model corresponding to each term in the SGS-scale (fluctuations) equation is correct.

References:

- [1] CHOU P Y, CHOU R L. 50 years of turbulence research in China[J]. *Annual Review of Fluid Mechanics*, 1995, **27**: 1-15.
- [2] CHOU P Y. On an extension of Reynolds' method of finding apparent stress and the nature of turbulence[J]. *Acta Physica Sinica*, 1940, **4**(1): 1-34.
- [3] FU S, WANG L. *Theory of Turbulence Modelling*[M]. Beijing: Science Press, 2023.
- [4] GARNIER E, ADAMS N, SAGAUT P. *Large Eddy Simulation for Compressible Flows*[M]. New York: Springer, 2009.
- [5] SPALART P R. Strategies for turbulence modelling and simulations[J]. *International Journal of Heat and Fluid Flow*, 2000, **21**: 252-263.
- [6] FU D X, MA Y W, LI X L, et al. *Direct Numerical Simulation of Compressible Turbulence*[M]. Beijing: Science Press, 2010.
- [7] WU C J, GUAN H, ZHAO H L. Large eddy simulation method based on small-scale SGS model, new development and applications of turbulence theory[C]//*New Developments of Turbulence Theory and Applications*. Shanghai: Shanghai University Press, 2000: 76-82.
- [8] GUAN H, WU C J. Large-eddy simulations of turbulent flows with lattice Boltzmann dynamics and dynamical system sub-grid models[J]. *Science in China Series E: Technological Sciences*, 2009, **52**(3): 670-679.
- [9] QI J, WU C J. Construction of spatiotemporal-coupling optimal low-dimensional dynamical systems for compressible Navier-Stokes equations[J]. *Applied Mathematics and Mechanics*, 2022, **43**(10): 1053-1085.
- [10] BASSE N T. Turbulence intensity scaling: a fugue[J]. *Fluids*, 2019, **4**(4): 180.
- [11] BASSE N T. Scaling of global properties of fluctuating and mean streamwise velocities in pipe flow: characterization of a high Reynolds number transition region[J]. *Physics of Fluids*, 2021, **33**: 065127.
- [12] TRITSCHLER V K, HICKEL S, HU X Y, et al. On the Kolmogorov inertial subrange developing from Richtmyer-Meshkov instability[J]. *Physics of Fluids*, 2013, **25**: 071701.
- [13] COURANT R, FRIEDRICHS K O. *Supersonic Flow and Shock Waves*[M]. New York: Interscience, 1948.